Infrared Physics & Technology 131 (2023) 104677

Contents lists available at ScienceDirect

Infrared Physics and Technology

journal homepage: www.elsevier.com/locate/infrared

Portable near-infrared spectral imaging combining deep learning and chemometrics for dry matter and soluble solids prediction in intact kiwifruit

Puneet Mishra [a,b,*], Jan Verschoor [b], Mariska Nijenhuis-de Vries [b], Gerrit Polder [a,c], Martin P. Boer [d]

[a] Agro-Food Robotics, Wageningen University & Research, the Netherlands
[b] Wageningen Food and Biobased Research Wageningen University & Research, the Netherlands
[c] Greenhouse Horticulture, Wageningen University & Research, the Netherlands
[d] Biometris, Wageningen University & Research, the Netherlands

ARTICLE INFO

Keywords:
Artificial intelligence
High throughput
Non-destructive
Fruit analysis

ABSTRACT

A novel case of developing a portable spectral imaging device for kiwifruit analysis is presented. Furthermore, a new complementary spectral image processing strategy combining deep learning and advanced chemometric is proposed for processing the spectral images. The deep learning was used for detection and localisation of harvested fruit in the spectral image while the chemometric modelling was used to predict multiple fruit quality related properties i.e., dry matter and soluble solids content. The developed models were independently validated on fruit harvested from a different orchard as well as on a different variety. The one touch spectral imaging presented in this paper can allow widespread usage of spectral imaging for fresh fruit analysis, particularly benefitting non-experts in spectral imaging and chemometrics to routinely use the spectral imaging for fresh fruit analysis.

1. Introduction

Optical spectral techniques are widely used for fresh fruit analysis [1,2]. One of the most common spectral technique is the visible and near-infrared (Vis-NIR) spectroscopy [3,4]. The Vis-NIR (400–1100 nm) is based on the interaction of the electromagnetic radiation (EMR) with the fruit and recording phenomena such as reflection, transmission, and absorption of EMR [5]. Although different types of spectral techniques are interesting for fruit analysis [2], however, the Vis-NIR techniques has some unique advantages for being preferred over other spectral techniques. For example, the Vis-NIR EMR detector and complete sensing solutions as point spectrometers (both lab-based and handheld) are readily available in the market [3]. Furthermore, the Vis-NIR sensing utilises the silicon-based detectors which are lower in cost compared to the detectors used for other sensing modalities such as short-wave infrared. Also, in some studies [6] it has been shown that the light penetration beneath the fruit skin is the highest for the NIR part of EMR bringing back more detailed information from the fruit. The light penetration is higher in the NIR part as the water absorption coefficient is lower [5,6].

In the current state of the art, there are two main modalities of Vis-NIR spectral sensing that are widely deployed. The first is the point based spectral sensing where the Vis-NIR signals are recorded individually for each fruit and at a localised position on the fruit [4]. The second modality is the spectral imaging which measures the spatially distributed Vis-NIR spectral responses for fruit [7]. Both modalities are complementary and are useful for non-destructive fruit analysis at different levels of fresh fruit chain. For example, the point-based sensing which is available in portable, or pocket forms is highly suitable for measuring fresh fruit during their early stages such as while the fruit are still on tree or plant [8,9]. This is possible as the portable spectrometer can be brought close to the fruit in tree or plant without any need to pluck the fruit from tree, leading to minimal fruit wastage as well no need for chemical destructive analysis, enabling monitoring development in time on individual fruits. However, one can assume that point spectral modality may not be an ideal approach when it comes to high-throughput analysis of fruit, where many fruits need to be analysed in a fast way. In such a scenario combined spectral and spatial sensing, aka spectral

* Corresponding author.
E-mail address: puneet.mishra@wur.nl (P. Mishra).

https://doi.org/10.1016/j.infrared.2023.104677
Received 25 July 2022; Received in revised form 25 March 2023; Accepted 30 March 2023
Available online 7 April 2023

Table 1
A summary of total number of fruit samples (=fruits) used for the experiment. Note that the dry matter band indicates the preliminary classification of fruit into groups based on estimated increasing dry matter; the individual fruit were experimentally assessed for DM as part of this study and verified in the results section.

Type	Dry matter band	Fruit Orchard A	Fruit Orchard B	Fruit Orchard C
Green	1	10	10	10
Green	2	10	10	10
Green	3	10	10	10
Green	4	10	10	10
Green	5	10	10	10
Green	6	10	10	10
Gold	4 & 5	10	10	10
Total samples	210			

imaging, can be used to quickly scan multiple fruits simultaneously [7,10]. Another benefit of spectral imaging is that it provides spatial information which can provide insights to the distribution of properties as a function of fruit surface [11], or improves estimation of individual fruit values compared to spot measurements.

Although the point spectroscopy for fruit analysis in terms of instrumentation is fairly developed and a wide range of easy-to-use portable instruments for fruit analysis is available in the market [3,12], the developments in the spectral imaging in terms of easy-to-use instruments are still limited. In the current state of the art, users need to purchase individual components and build the imaging systems by their own. Such a system development is suitable for scientific practitioners, but the main impact spectral sensing can have when the spectral instruments are used by real-life fruit growers and handlers. Unfortunately for spectral imaging, this is currently far from common practise.

In past many years, there has been extensive research on the application of fresh fruit analysis with spectral imaging [7]. In many works, it has been demonstrated that spectral imaging can allow fast and non-destructive analysis of fresh fruits [13]. Application ranges from qualitative analysis such as bruise and defects detection to prediction of chemical components such as dry matter (DM) and soluble solids content (SSC) [7,13]. However, as highlighted earlier, most of the studies were performed as sophisticated scientific experiments and with customised spectral imaging systems with minimal focus on the practical applicability of the technique.

In this study, a novel case of developing one touch portable spectral imaging for kiwifruit analysis. The backbone of the approach was the All-In-One spectral imaging (ASI) [10] framework for standardised and controlled spectral imaging and real-time model deployment. Furthermore, a new complementary strategy combining deep learning and advanced chemometrics is proposed for processing the spectral images of fresh fruit. The deep learning was used for detection and localisation of fruit in the spectral image while the chemometric modelling was used to predict multiple fruit properties i.e., DM and SSC. The developed models were independently validated on fruit harvested from different orchards as well as on a different variety.

2. Material and methods

2.1. Fruit samples

The fruit samples were provided by Zespri, New Zealand, batches of Gold kiwifruit (A. *chinensis* var. chinensis 'Zesy002') and Green kiwifruit (A. *chinensis* var. *deliciosa* 'Hayward') were provided by Zespri (New Zealand) from three orchards, in the Bay of Plenty region, harvested at

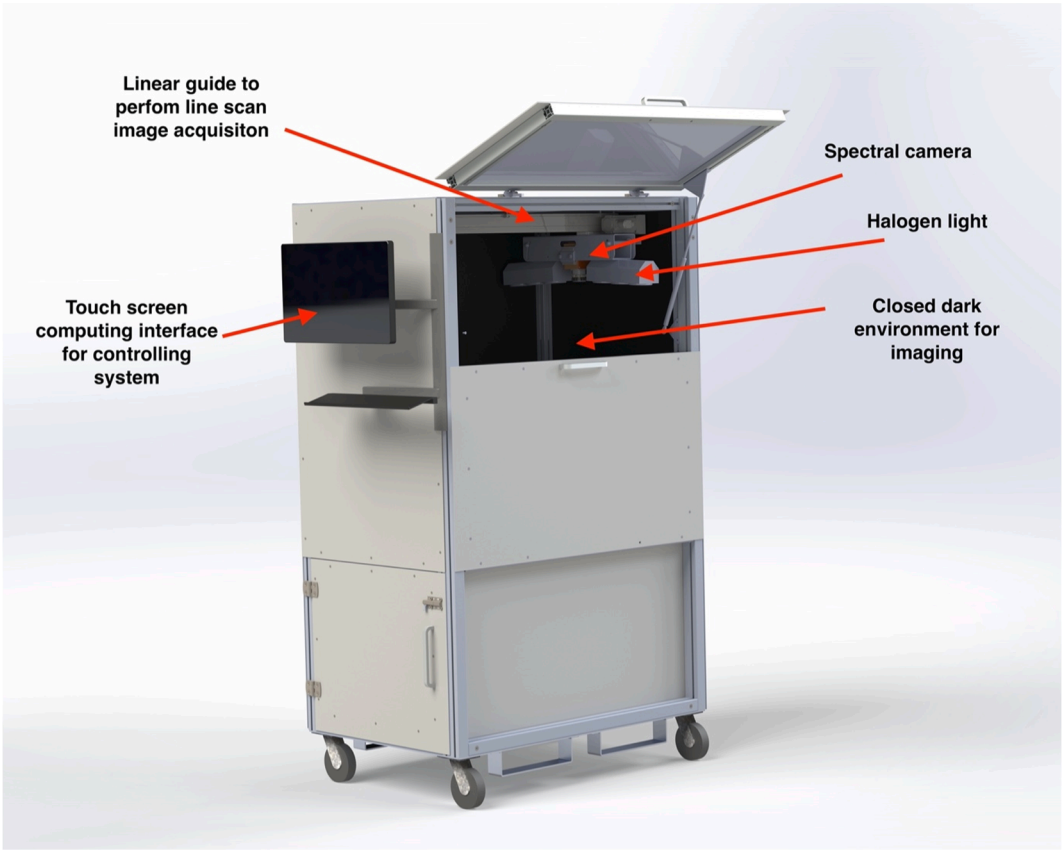

Fig. 1. The all-in-one spectral imaging (ASI) setup for standardized spectral imaging [15]. The ASI allows automatic image acquisition as well as automatic radiometric correction of the images using white and dark reference.

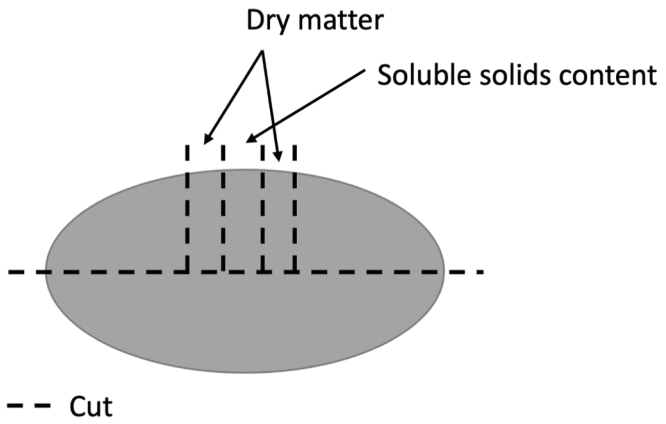

Fig. 2. A schematic of the sampling points for reference measurements performed on the Kiwifruit.

different stages to achieve batches with six projected dry matter (DM) ranges. The three orchards will be denoted as A, B and C in this study due to the commercial confidentiality of the orchards. DM is the solid component of the fruit, i.e., what is left after all the water is removed. The fruit were shipped to Europe in containers and transported to the Netherlands by road transport stored at 1 °C and ripened up to approx. 0.5–0.8 kgf penetrometer value (using 8 mm diameter probe) in the post-harvest facilities of Wageningen Food & Biobased Research, The Netherlands. Before the experimental day, fruit were left atroom temperature conditions overnight to stabilise the temperature for spectral imaging. The sample details are provided in Table 1. For simplification and anonymisation, orchards are denoted as orchards A, B and C.

2.2. Spectral imaging

Spectral images of kiwifruit were recorded with the recently developed ASI setup [10,14,15] at Wageningen Food & Biobased Research, The Netherlands (Fig. 1). ASI setup uses a Vis-NIR spectral camera (Fx10, Specim, Oulu, Finland) for automatic spectral image acquisition. The camera records data in the spectral range of 398–1000 nm with a spectral interval of ~ 3 nm. In ASI, the samples are illuminated with two sets of halogen lights (supplied by Specim, Oulu, Finland) mounted next to the spectral camera (Fig. 1). The distance to the white reference and the samples is always the same as well as the travel distance of the camera mounted on the linear guide, hence, no changes in the settings during image acquisition are required. The software of the ASI setup is in-house developed at Wageningen Food & Biobased Research, The Netherlands, allowing a fully automated image acquisition and the acquisition controls such as the speed of the translation stage, exposure time, number of frames, etc. are pre-synchronised with the camera settings [10]. The speed of transalation stage was 30 mm/*sec*. The exposure time was 0.02 *sec*. The distance of sensor from fruit was ~ 600 mm. Automatic radiometric correction using white and dark references is also integrated in the software. For white reference, the ASI setup has an inbuilt white reference (Teflon) (Fig. 1) while for dark reference the camera allows automatic shutter control to record the dark reference. The output from the ASI system is the reflectance image.

2.3. Reference measurements

Manual sampling was performed on the kiwifruit (A schematic of the sampling locations on the fruit is shown in Fig. 2.). The reference measurements were dry matter (DM) and soluble solids content (SSC). DM for kiwi was determined using an electronic balance XS10001 L (Mettler-Toledo GmbH, Giessen, Germany) by recording the weight of the parts before and after drying in a food dehydrator (Ezidri, Hydraflow Industies ltd., New Zealand) at 65 °C for 24 h. SSC was determined using a handheld refractometer (PAL-1, Atago, Japan). All reference measurements were performed at room temperature.

2.4. Spectral image processing

In this study, a novel combination of deep learning and chemometric modelling to process the spectral images as demonstrated in earlier work [15]. The main aim was to automate the image analysis so that any user with minimal experience in data modelling and spectroscopy could use the imaging system for fruit analysis. The image analysis included a two-step process.

1. Step 1 - Used deep learning to detect individual fruit in the imaged scene.
2. Step 2 - Used pixels corresponding to individual fruit to apply the chemometric model for prediction of fruit properties.

Deep learning was not used for the prediction of chemical properties as the number of fruits for training a deep learning model was too low.

2.4.1. Deep learning-based fruit detection

In this study, the deep learning model YOLOv4 developed in earlier study was used to detect kiwifruit [15]. All analysis were conducted in the MATLAB computing environment (release R2021a, The MathWorks, Inc., Natick, MA, USA) using the open-source scripts downloaded from: *https://github.com/matlab-deep-learning/pretrained-yolo-v4*. The aim of fruit detection was to locate individual fruit such that the spectra for the fruit can be accessed without needing any manual Region of Interest (ROI) selection. The spectra extracted for the detected kiwifruit were used for chemometric modelling and later model testing. The YOLOv4 model was applied on the RGB images reconstructed using the spectral bands 671, 534, and 430 nm of the spectral image. The outputs of the YOLOv4 are the bounding boxes, centroids, and probability score for detection of kiwifruit. The centroids were used to extract the spectra for the fruit which were later used for chemometric modelling to predict the DM and SSC. Since Kiwi is a symmetrical fruit hence the centroid estimated by the deep learning model present the exact center of the fruit. Note that mean spectra were extracted inside the window of pre-defined width to study the effect of window width on the model performance. In total, 13 different window options were explored i.e., 1–25 in the interval of 2.

2.4.2. PLS modelling

The chemometric partial least-squares modelling [16,17] was performed using the mean spectra estimated using the centroid locations predicted by the deep learning model. Please note that since this study aimd to jointly model the DM and SSC in the same model, hence, the actual modelling was the PLS2 [17] modelling suitable for handling multiple responses. This study explored both the raw reflectance and standard normal variates (SNV) [18] normalized reflectance to understand if normalization have any benefit on the modeling. This study also explored two spectral ranges, i.e., 500–1000 nm and 688–1000 nm, to see the benefit of having color information in the model (500–1000 nm) compared to only using the NIR information (688–1000 nm). Note that the spectral information below 500 nm was not used due to noise. Note that there were a total of 120 green kiwi samples (Orchard A and B) in the calibration set, 60 green kiwi (Orchard C) samples in the test set for a different orchard, and 30 gold kiwi samples for a different variety. To decide the optimal number of components for the PLS model, 5-fold cross-validation was used. The optimal components were identified as those carrying the lowest cross-validation error. Once the optimal model was found, the model was independently tested on data from a new orchard and a new variety. The performance of the models was evaluated using the root mean squared error of prediction (RMSEP).

Table 2
A summary of reference dry matter and soluble solids content (mean ± standard deviation) in different kiwifruit samples.

Property	Green kiwifruit			Gold kiwifruit
	Orchard A	Orchard B	Orchard C	
Dry matter (%)	17.22 ± 1.85	16.87 ± 1.89	16.87 ± 1.94	17.43 ± 0.72
Soluble solids (%)	14.14 ± 1.77	13.88 ± 1.73	13.76 ± 1.75	15.42 ± 0.65

3. Results and discussion

3.1. Reference data

A summary of the reference DM for different kiwifruit samples is shown in Table 2. The DM range for the kiwifruit (both the green and gold kiwifruit) were similar. The mean SSC for gold kiwifruit was higher with a narrower standard deviation compared to the green kiwifruit. A lower standard deviation for gold kiwifruit is due to a smaller sample size than green kiwifruit (i.e. 30 fruit/orchard vs 60 fruit/orchard). Due to the low number of fruit samples, the gold kiwifruit was left out of data modelling, but was used for independent testing of the chemometric model to predict DM and SSC.

3.2. Deep learning-based object detection and mean spectra extraction

The results of the application of YOLOv4 object detector for detecting green and gold kiwifruit are shown in Fig. 3A and 3B, respectively. Note that the deep learning model was applied in the RGB images reconstructed from the spectral images. In this study, no training or fine-tuning of the deep learning models was perfomed as the model was used directly from earlier study [15]. For both the green and gold kiwifruit, all fruit were detected correctly (marked in red Fig. 3) with detection probability > 85 %, and their centroids were correctly identified. Using the centroid location identified with deep learning, the mean spectra with varying window widths (spatial pixels) were extracted. An example of the mean spectra with varying window width is shown in Fig. 4. Furthermore, the spectra are presented before (A) and after (B) SNV normalisation. As the window width for estimating mean spectra

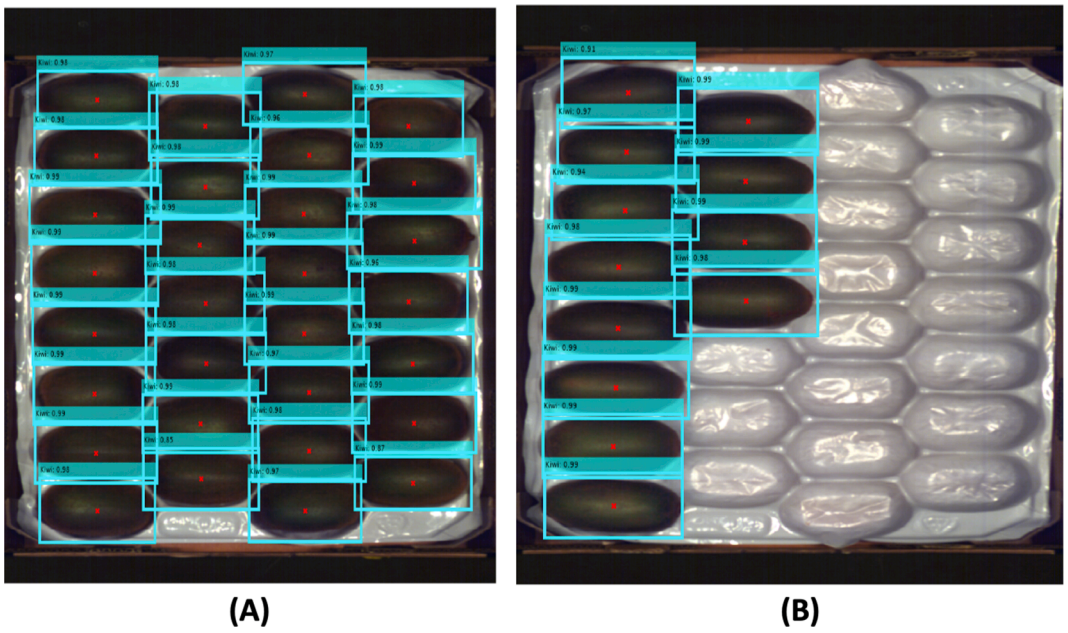

Fig. 3. Results of detecting green (A) and gold (B) kiwifruit by application of YOLOv4 deep learning model developed in earlier study [15]. (For interpretation of the references to color in this figure legend, the reader is referred to the web version of this article.)

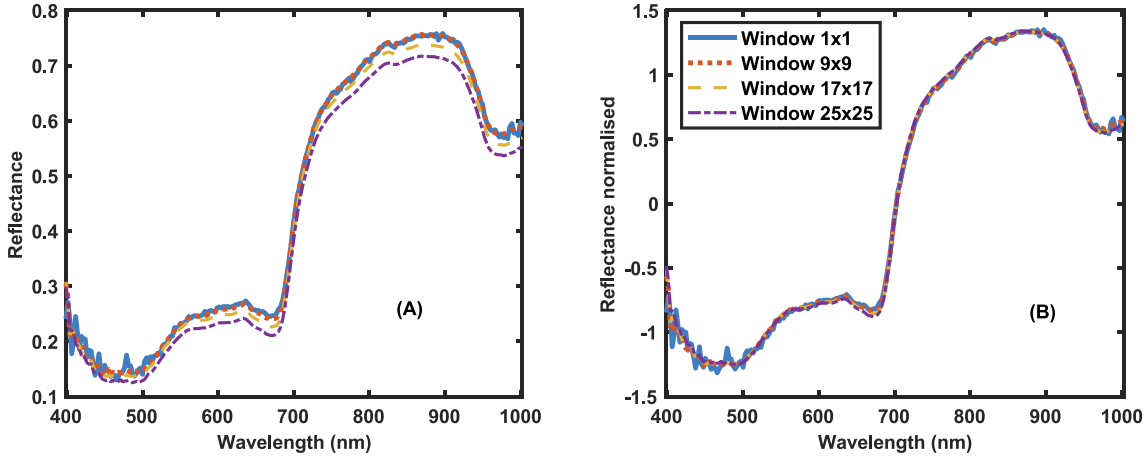

Fig. 4. The effect of changing window width for estimating the mean spectra. (A) Reflectance, and (B) standard normal variate normalised reflectance.

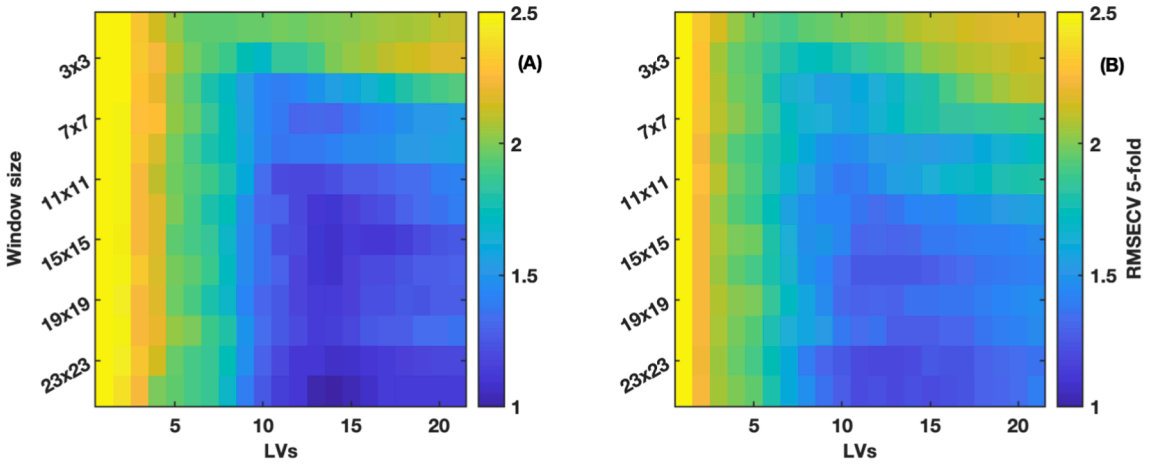

Fig. 5. Root mean squared error of cross-validation (RMSECV) maps for cross-validation analysis performed on data in spectral range of 500–1000 nm. (A) Reflectance, and (B) Standard normal variate normalised reflectance. In x-axis explains the number of latent variables (LVs) and y-axis is the window width explaining the number of pixels used for estimating mean spectra.

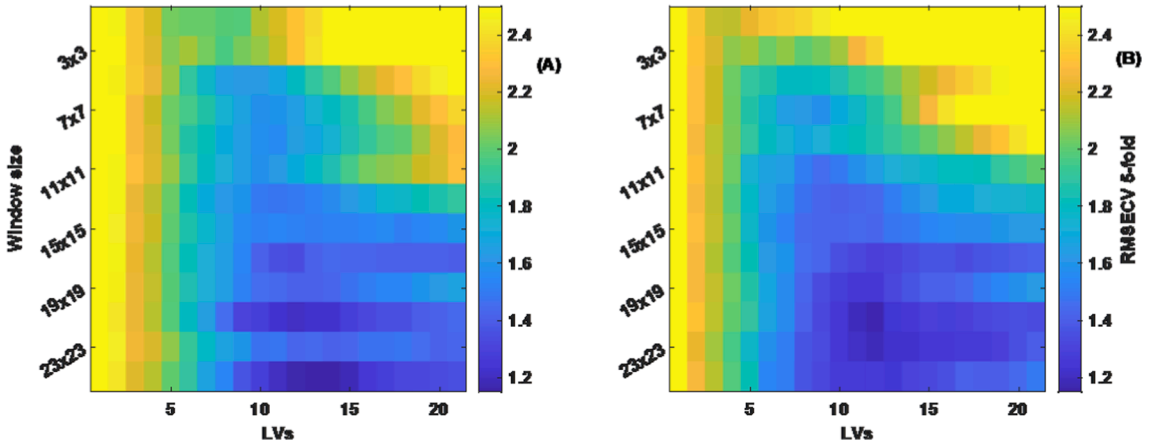

Fig. 6. Root mean squared error of cross-validation (RMSECV) maps for cross-validation analysis performed on data in spectral range of 688–1000 nm. (A) Reflectance, and (B) Standard normal variate normalised reflectance. In x-axis explains the number of latent variables (LVs) and y-axis is the window width explaining the number of pixels used for estimating mean spectra.

increased, the noise in the spectra was reduced, particularly noticeable in range of 400–500 nm in Fig. 4A. The other observation noted was that with the increasing window width, the overall intensity of the reflectance signal decreased (Fig. 4A). This overall reduction could be that as the window size increases the spectra correspond to the curved part of the kiwifruit were included for the estimation of mean. Since the curved part is at a far distance compared to the top part, hence, the addition of spectra corresponding to the curved part can reduce the overall spectral signal intensity. However, if needed such overall difference in signal intensity can be normalised with the SNV normalisation (Fig. 4B). Due to less noise in the spectra obtained as the mean of pixels in a larger window width, it can be expected that the model performance should also be better for the mean spectra obtained with larger window width (verified in the next section).

3.3. PLS2 analysis for joint prediction of dry matter and soluble solids content

PLS2 modelling was performed to jointly predict the DM (Fig. 5) and SSC (Fig. 6) in kiwifruit. As a first step for model development, the 5-fold cross-validation analysis was performed to identify the optimal number of latent variables (LVs) and window width for estimating the mean spectra. Furthermore, the analysis was performed for both the reflectance (Fig. 5A) and the SNV normalised reflectance data (Fig. 5B). The lowest RMSECV (0.99 %) was obtained using the reflectance data compared to the RMSECV (1.18 %) for SNV normalised data. Hence, due to lower RMSECV, the final models were calibrated on the reflectance data estimated with the window size of 25 × 25 and 13 LVs. In general, a smaller window width for estimating mean spectra results in higher RMSECV than with bigger window width.

Data analysis was also perfomed by reducing the spectral range to 688–1000 nm. In other words, the visible information (400–688 nm) was removed from data and model based solely on NIR data were explored to find if NIR spectral range alone is sufficient to predict the DM and SSC. Variable reduction was also perfomed to see if the model based on green kiwifruit using only the NIR information can predict the DM and SSC in gold kiwifruits the outer peel colours for both kiwifruit are different and may influence the performance of the model calibrated on the data including colour information. While comparing the RMSECV for reflectance and normalised data, the lowest RMSECV (1.15 %) was related to the reflectance data, hence, the reflectance data were selected to develop the final models. The final models were calibrated on the reflectance data estimated with the window size of 25 × 25 and 13 LVs. As can be understood that for both the modelling cases, the lowest RMSECV was achieved with the raw reflectance data, while the RMSECV was higher for the normalised data. This finding is aligned with a recent

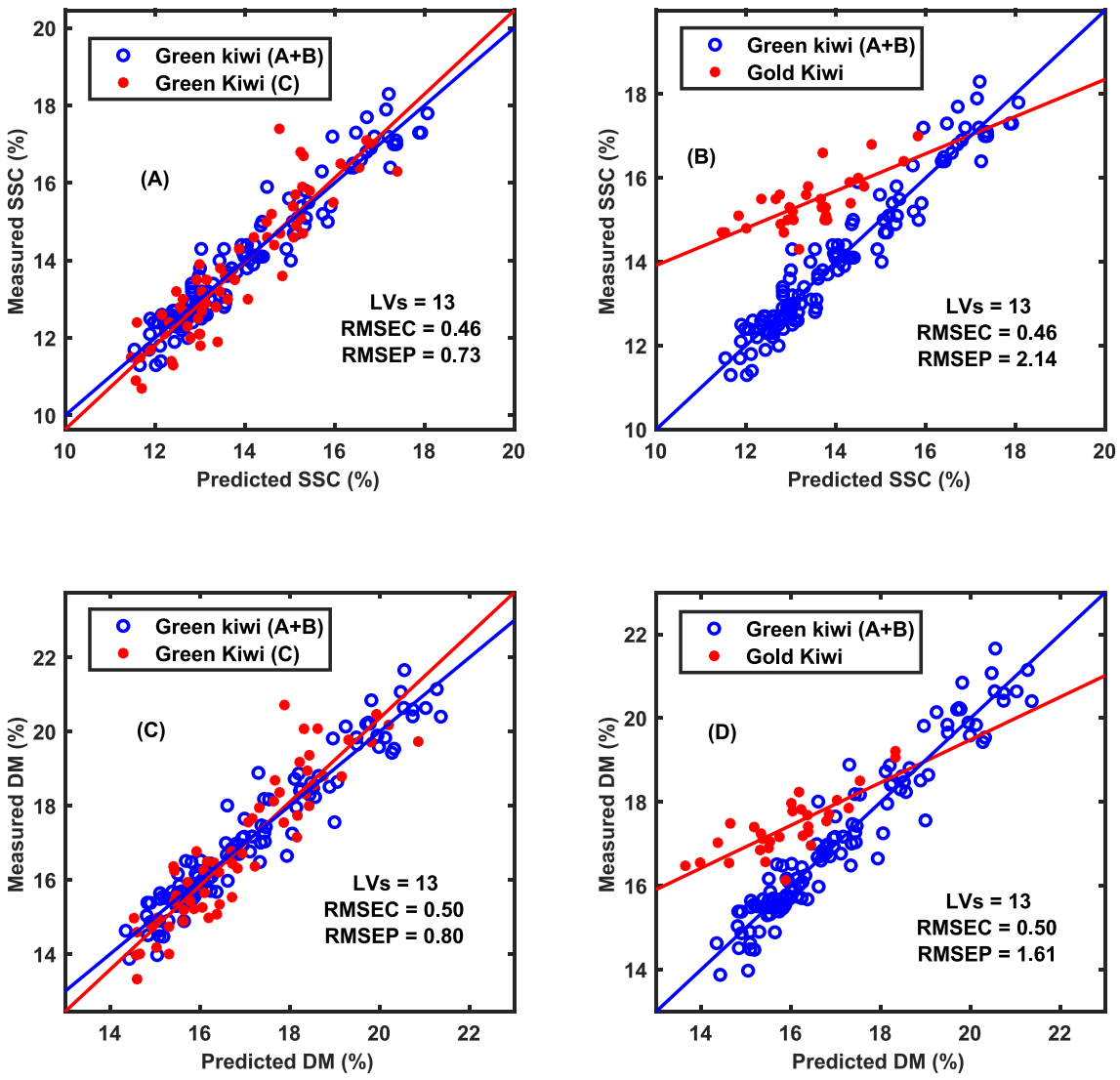

Fig. 7. Prediction plots for dry matter (DM) and soluble solids content (SSC) for modelling performed in spectral range of 500–1000 nm. For green kiwifruit, the model was made on two orchards (A + B) and tested on one orchard (C). (A) SSC prediction on data from new orchards, (B) SSC prediction on data from gold kiwifruit, (C) DM prediction on data from new orchards, and (D) DM prediction on data from gold kiwifruit. (For interpretation of the references to color in this figure legend, the reader is referred to the web version of this article.)

study which concluded that spectral pre-processing may not be needed for fresh fruit as they may eliminate the useful information present in reflectance spectral data related to light scattering [19]. From the cross-validation analysis performed on the data having the colour + NIR information (500–1000 nm) and having only NIR information (688–1000 nm), it was found that the RMSECV was the lowest when the colour information was included in the model. This gives an indication that the colour information is of use for predicting DM and SSC in green kiwifruit.

The performance of the final PLS2 models for spectral ranges of 500–1000 nm and 688–1000 nm are shown in Figs. 7 and 8, respectively. For both the DM and SSC, the RMSEP were lower than 1 %, which is the usual range of error for NIR technology [20–22]. The model performance was poor for predicting the DM and SSC in gold kiwifruit, particularly having poor slope rather than the commonly encountered bias shifts. It was noted that the performances of models for predicting DM and SSC in green kiwifruit from a different orchard were better using the spectral range of 500–1000 nm compared to the spectral range of 688–1000 nm. For example, the RMSEP = 0.73 % was achieved with the model developed using 500–1000 nm compared to RMSEP = 0.88 % achieved with the model developed using 688–1000 nm spectral range. Similar results were noted also for the SSC. Better model performance with 500–1000 nm spectral range confirms that the colour information can be of use for predicting the DM and SSC in kiwifruit. For Gold kiwifruit, both the spectral ranges had a similar overall performance. Initially, the assumption was that a green kiwifruit model based solely on the NIR information may perform better than the model made using colour + NIR information, however, the differences were minimal in terms of RMSEP. Furthermore, looking at the predictions scatter plots it was noted that the predictions have more spread when only the NIR information was used in the modelling, compared to using the colour + NIR information. Overall, the models based on green kiwifruit cannot directly predict the properties of gold kiwifruit. There are many reasons which could be related to this such as different physical structures outside the peel, for example, the green kiwifruit has hairy peel which can interact differently with the Vis-NIR light compared to the non-hairy peel of the gold kiwifruit. In practice, different models should be created for different kiwifruit varities/ cultivars. Altough in presence of data from several kiwifruit varities/ cultivars, it is advisable to develop global models as recently performed in a recent study related to mango fruit [8,9]. However, developing global models was out of scope in this work due to limited sample size and will be explored in future works.

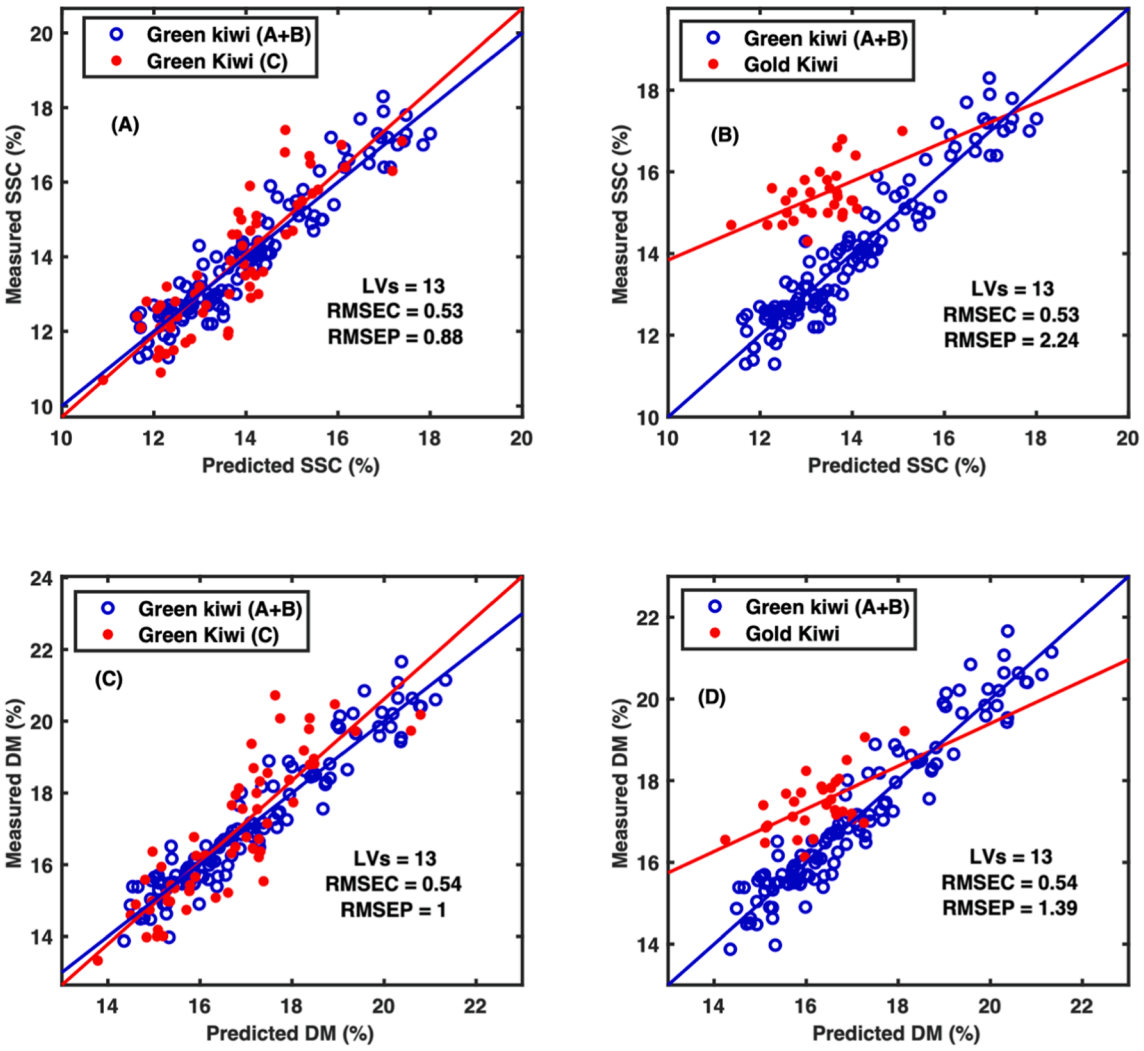

Fig. 8. Prediction plots for dry matter (DM) and soluble solids content (SSC) for modelling performed in spectral range of 688–1000 nm. For green kiwifruit, the model was made on two orchards (A + B) and tested on one orchard (C). (A) SSC prediction on data from new orchards, (B) SSC prediction on data from gold kiwifruit, (C) DM prediction on data from new orchards, and (D) DM prediction on data from gold kiwifruit. (For interpretation of the references to color in this figure legend, the reader is referred to the web version of this article.)

3.4. Example demonstrative application

One of the aims of this study was to develop a push button approach to spectral imaging for kiwifruit analysis. In that regard, this study relied on the ASI system for spectral image acquisition while for the processing of the data a combination of deep learning and chemometric modelling was proposed. To demonstrate how such an approach to spectral imaging looks like in practice an example prediction image is show in Fig. 9. In Fig. 9A, the RGB image reconstructed from spectral imaging for a box of kiwifruit is shown. In Fig. 9B, the sample image with fruit detection and simultaneous fruit property prediction is shown. The bound box in Fig. 9B indicates a detected fruit and the description of predicted DM and SSC is presented in the head of the bounding box. The overall process of image acquisition to deployment of the model was tested, and it took less than 30 s.

4. Conclusion

The study demonstrated a real case of simplifying the spectral imaging and associated image processing to predict fruit properties. Furthermore, kiwifruit analysis was used to show the potential of the proposed approach. This study built over the framework of the All-In-One spectral imaging by adding deep learning and chemometric models for kiwifruit. Deep learning allowed the identification and localisation of the kiwifruit while the chemometric modelling was used for predicting DM and SSC. With the independent test of the model on data from new orchard and variety, it was found that the spectral models (made on green kiwifruit) worked well on the data from green kiwifruit but performed poorly for data from gold kiwifruit. The reason for failure of the model test on could be the very different peel structures of green and gold kiwifruit. It was noted that having a larger area (more pixels) for estimating fruit mean spectra led to lower prediction errors compared to using a smaller area (less pixels). Spectral models were found to be in general better when developed directly using the reflectance data and their performance decreased when the spectra were pre-processed with spectral normalisation such as SNV. The initial assumption that only using the NIR information for developing models for green kiwifruit may work also for gold kiwifruit was not fully correct, as it was noted that the model performance with NIR and colour + NIR information were similar when tested on gold kiwifruit. However, the performance of the model (based on only NIR) was poorer for green kiwifruit indicating that both colour and NIR information may play a crucial role for predicting DM and SSC in green kiwifruit. In terms of achieving generalised chemometric models, it is advised to measure data from wide kiwifruit variety/cultivars and develop global models. In relation to simplifying the spectral imaging for other fruit types, the ASI

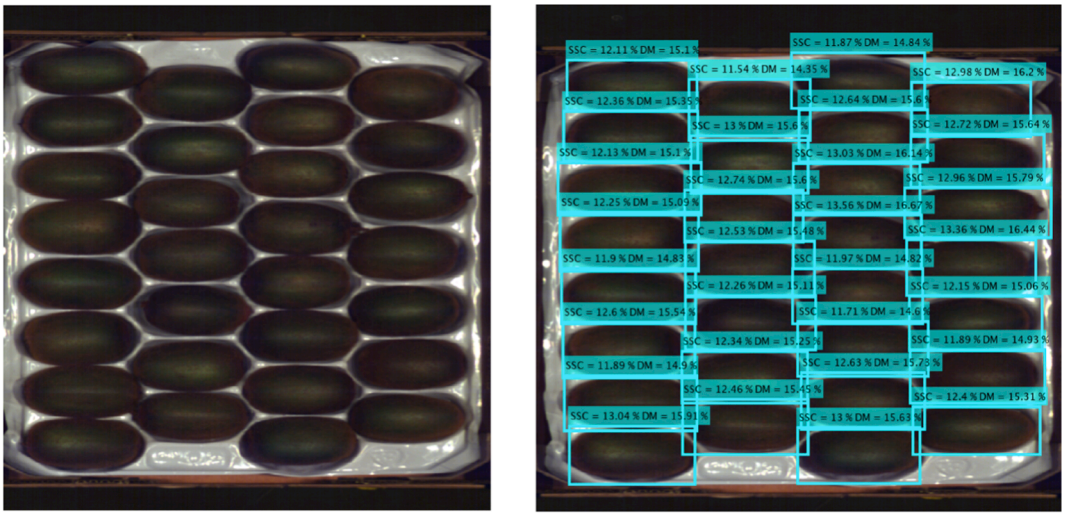

Fig. 9. An example prediction from the joint deep learning-based kiwifruit detection and PLS2 model based dry matter and soluble solids prediction in Kiwifruit. (A) RGB image reconstructed from spectral image, and (B) Image with bounding boxes explaining the dry matter and soluble solids content of each fruit.

system can be combined with models of any fruit without any change in the hardware.

Declaration of Competing Interest

The authors declare that they have no known competing financial interests or personal relationships that could have appeared to influence the work reported in this paper.

Data availability

Data will be made available on request.

Acknowledgments

Authors would like to thanks Zespri, New Zealand for providing Kiwifruits used in this study.

This research was supported by the Wageningen University & Research knowledge base program 'Data Driven & High Tech.

References

[1] G.P. Moreda, et al., Non-destructive technologies for fruit and vegetable size determination – a review, J. Food Eng. 92 (2) (2009) 119–136.
[2] H.L. Wang, et al., Fruit quality evaluation using spectroscopy technology: a review, Sensors 15 (5) (2015) 11889–11927.
[3] K.B. Walsh, V.A. McGlone, D.H. Han, The uses of near infra-red spectroscopy in postharvest decision support: a review, Postharvest Biol. Technol. 163 (2020), 111139.
[4] B.M. Nicolai, et al., Nondestructive measurement of fruit and vegetable quality by means of NIR spectroscopy: a review, Postharvest Biol. Technol. 46 (2) (2007) 99–118.
[5] K.B. Walsh, et al., Visible-NIR 'point' spectroscopy in postharvest fruit and vegetable assessment: the science behind three decades of commercial use, Postharvest Biol. Technol. 168 (2020), 111246.
[6] J. Lammertyn, et al., Light penetration properties of NIR radiation in fruit with respect to non-destructive quality assessment, Postharvest Biol. Technol. 18 (2) (2000) 121–132.
[7] Y. Lu, et al., Hyperspectral imaging technology for quality and safety evaluation of horticultural products: a review and celebration of the past 20-year progress, Postharvest Biol. Technol. 170 (2020), 111318.
[8] X.D. Sun, P. Subedi, K.B. Walsh, Achieving robustness to temperature change of a NIRS-PLSR model for intact mango fruit dry matter content, Postharvest Biol. Technol. 162 (2020).
[9] N.T. Anderson, et al., Achieving robustness across season, location and cultivar for a NIRS model for intact mango fruit dry matter content. II. Local PLS and nonlinear models, Postharvest Biol. Technol. 171 (2021), 111358.
[10] P. Mishra, et al., All-in-one: a spectral imaging laboratory system for standardised automated image acquisition and real-time spectral model deployment, Anal. Chim. Acta 1190 (2022), 339235.
[11] T. Ma, et al., Noncontact evaluation of soluble solids content in apples by near-infrared hyperspectral imaging, J. Food Eng. 224 (2018) 53–61.
[12] R.A. Crocombe, Portable spectroscopy, Appl. Spectrosc. 72 (12) (2018) 1701–1751.
[13] N.-N. Wang, et al., Recent advances in the application of hyperspectral imaging for evaluating fruit quality, Food Anal. Methods 9 (1) (2016) 178–191.
[14] P. Mishra, Deep generative neural networks for spectral image processing, Anal. Chim. Acta (2021), 339308.
[15] J. Xu, P. Mishra, Combining deep learning with chemometrics when it is really needed: a case of real time object detection and spectral model application for spectral image processing, Anal. Chim. Acta (2022), 339668.
[16] Wold, S., PLS Modeling with Latent Variables in Two Or More Dimensions. 1987.
[17] S. Wold, M. Sjostrom, L. Eriksson, PLS-regression: a basic tool of chemometrics, Chemom. Intel. Lab. Syst. 58 (2) (2001) 109–130.
[18] R.J. Barnes, M.S. Dhanoa, S.J. Lister, Standard normal variate transformation and De-trending of near-infrared diffuse reflectance spectra, Appl. Spectrosc. 43 (5) (1989) 772–777.
[19] P. Mishra, et al., Chemometric pre-processing can negatively affect the performance of near-infrared spectroscopy models for fruit quality prediction, Talanta (2021), 122303.
[20] P. Mishra, E. Woltering, Handling batch-to-batch variability in portable spectroscopy of fresh fruit with minimal parameter adjustment, Anal. Chim. Acta 1177 (2021), 338771.
[21] T. Ma, et al., Rapid and nondestructive prediction of firmness, soluble solids content, and pH in kiwifruit using Vis–NIR spatially resolved spectroscopy, Postharvest Biol. Technol. 186 (2022), 111841.
[22] T. Ma, et al., Non-destructive and fast method of mapping the distribution of the soluble solids content and pH in kiwifruit using object rotation near-infrared hyperspectral imaging approach, Postharvest Biol. Technol. 174 (2021), 111440.